D. KALISZ, P. L. ŻAK, J. LELITO, M. SZUCKI, J. S. SUCHY, B. GRACZ

ISSN 0543-5846
METABK 54(1) 139-142 (2015)
UDC – UDK 669.15.782:669.74:661.249=111

MODELING OF MnS PRECIPITATION DURING THE CRYSTALLIZATION OF GRAIN ORIENTED SILICON STEEL

Received – Prispjelo: 2014-02-05
Accepted – Prihvaćeno: 2014-08-20
Preliminary Note – Prethodno priopćenje

The process of manganese sulfide formation in the course of grain-oriented silicon steel solidification process is described in the paper. Fine dispersive MnS inclusions are grain growth inhibitors and apart from AlN inclusions they contribute to the formation of a privileged texture, i.e. Goss texture. A computer simulation of a high-silicon steel ingot solidification with the use of author's software has been performed. Ueshima model was adapted for simulating the 3 % Si steel ingot solidification. The calculations accounted for the back diffusion effect according to Wołczyński equation. The computer simulation results are presented in the form of plots representing the process of steel components segregation in a solidifying ingot and curves illustrating the inclusion separation process.

Key words: Grain oriented silicon steel, MnS precipitates, segregation, continuous casting of steel.

INTRODUCTION

The grain oriented high silicon steel typically has a Goss structure [1]. Such texture provides high magnetic properties of steel, i.e. high inductivity and low loss. The process in which this kind of steel is formed strongly depends on grain growth inhibitors in the form of nonmetallic inclusions, i.e. MnS, Cu_2S, SeS and Cu_2Se. Their chemical composition, size and dispersion determine the quality of the ready product. The MnS inclusions are formed while the steel solidifies, as a result of elemental segregation phenomena at the solidification front and further cooling of ingot. While heating up to the temperature of rolling the MnS inclusions are dissolved nearly completely during hot rolling and cooling [2].

The concentration of elements making up MnS inclusions is established while refining and supplementing chemical composition, when liquid steel is prepared for casting. During solidification of steel its constituents are segregated into solid and liquid phases. Sulfur has low solid/liquid phase partition coefficient (k = 0,05), which means that liquid steel will be enriched in sulfur over the crystallization process advancement [3].

Manganese sulfide may be precipitated on oxide inclusions formed at high temperatures. In the solidification process it is both liquid steel and liquid nonmetallic oxide inclusions which are enriched with sulfur [4]. The MnS inclusions from liquid oxides can be separated after the ingot is completely solidified. However, after the oxide phase transformes into solid state this process ceases. Therefore, the change of all liquid phase components should be accounted for in the complete description of manganese sulfide formation. The thermodynamic criterion of MnS inclusions formation refers to the actual state of liquid phase composition. The MnS inclusions can be formed only when the equilibrium solubility product is exceeded:

$$\mathrm{Mn + S = MnS}$$

$$\Delta G = -R \cdot T \cdot \ln K = -R \cdot T \cdot \ln \frac{a_{MnS}}{f_A \cdot f_{[B]} \%Mn \cdot \%S} \quad (1)$$

$$C^t_{L(Mn)} \cdot f_{Mn} \cdot C^t_{L(S)} \cdot f_S \geq Q_{L(MnS)} \quad (2)$$

where: R - gas constant / J mol^{-1}·K^{-1}, T - temperature / K, f_{Mn}, f_S - coefficients of steel components activity, $C^t_{L(S)}$ - sulfur concentration in liquid phase, $Q_{L(MnS)}$- solubility product.

STEEL CRYSTALLIZATION MODEL

The behavior of liquid steel components during solidification is described with the Ueshima model presented in [3,5-10]. This model accounts for the effect of solids precipitation from a liquid during dendritic crystallization when the heat is directionally discharged with back-diffusion. The magnitude of back-diffusion for a single component „i" of liquid steel is characterized by back-diffusion parameter α_i [11]:

$$\alpha_i = \frac{D_i \cdot t_S}{l^2} \quad (3)$$

where: D_i - coefficient of diffusion of a „i" component formed in a solid phase, l - advancement of solidification front, t_s- local time of solidification.

$$t_S = \frac{T_L - T_S}{(dT/dt)} \quad (4)$$

where: T_L – liquidus temperature, T_S – solidus temperature, $\frac{dT}{dt}$ - cooling rate.

D. Kalisz, P. L. Żak, J. Lelito, M. Szucki, J. S. Suchy, B. Gracz, AGH University of Science and Technology, Faculty of Foundry Engineering, Kraków, Poland

This model accounts for solidification of a layer disposed perpendicular to the axis of a flat ingot. The temperature during solidification changes from liquidus to solidus and the respective equations were taken [3,6]. It was assumed that the diffusion of a steel componenet in a liquid phase is very fast, which means that its concentration in this phase at time t is constant. The back-diffusion crystallization was defined from Wołczyński's equation [11]:

$$C_S^* = k \cdot C_0 \cdot \left[1 + \alpha \cdot k \cdot f_S - f_S\right]^{\frac{k-1}{1-\alpha \cdot k}} \qquad (5)$$

where: C_0 - initial concetration of solute in the liquid, C_S^* - concetration of a given solute in the solid phase, f_s - participation of solid phase (fraction of mass), k - equilibrium partition coefficient for solid/liquid phase interface.

The diffusion of a component in solid phase was described with the Fick Law [6]:

$$\frac{\partial C_i}{\partial t} = D \cdot \frac{\partial^2 C_i}{\partial x^2} \qquad (6)$$

The values of diffusion coefficients D in solid phase δ (ferrite) and equilibrium partition coefficient $k^{\delta/L}$ for steel elements were assumed after [8, 9].

Authors adapted a microsegregation model for describing phenomena taking place during solidification of a high silicon ingot cast on CCS machine. Assumption was made that steel solidified from the edge of the ingot towards its center. The crystallization of the ingot 220 mm thick was assumed, and the simulation was performed for half of this size, i.e. 110 mm.

RESULTS OF CALCULATIONS

Computer calculations were performed for equilibrium conditions between metallic and nonmetallic phases. The values of constant equilibria for the reaction of nonmetallic inclusions formation in the analyzed system were based on [5, 6, 8, 9, 12, 13]. The activity coefficients of steel fractions were calculated with the use of the Wagner–Chapman equation. The first-order reaction parameters were assumed after [9]. The activity of oxide phase fractions was established on the basis of a regular solution model, accounting for the reaction parameters after Ban-Ya [14] and Iwanciw [15]. The chemical composition of steel used for calculations is presented in Table 1.

Table 1 **Chemical composition of steels / wt %**

Steel	S	Mn	Si	Al	N	O
1	0,0015	0,25	3	0,015	0,015	0,0018
2	0,007	0,25	3	0,009	0,0097	0,0018
3	0,015	0,25	3	0,015	0,015	0,018

Calculations were performed for two cooling rates 100 / K min^{-1} and 500 / K min^{-1}. The results are plotted in Figures 1 to 6.

The rapid drops visible on S and Mn segregation plots represent the process of MnS inclusions formation. Manganese sulfide is generated at the cooling rates of 100 and 500 / K min^{-1}. The last three portions of liquid steel do not contain diluted sulfur because it was

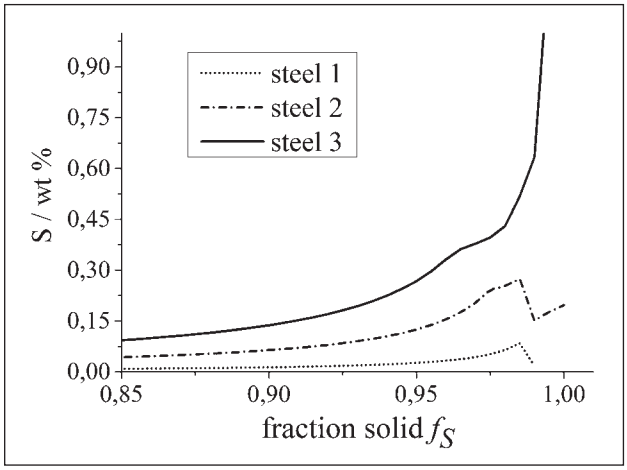

Figure 1 Sulfur segregation during silicon steel solidification at a cooling rate of 100 / K min^{-1}

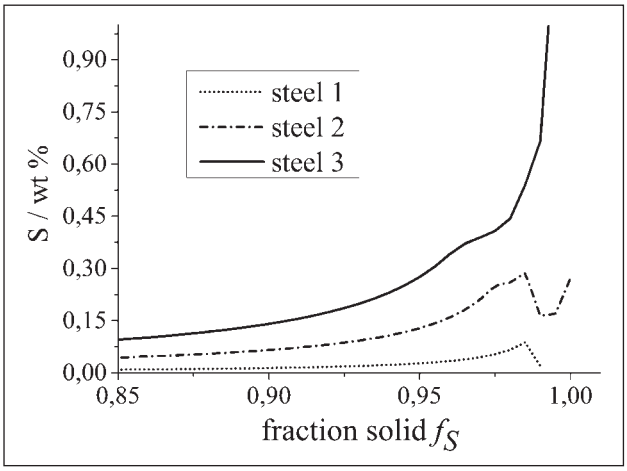

Figure 2 Sulfur segregation during silicon steel solidification at a cooling rate of 500 / K min^{-1}

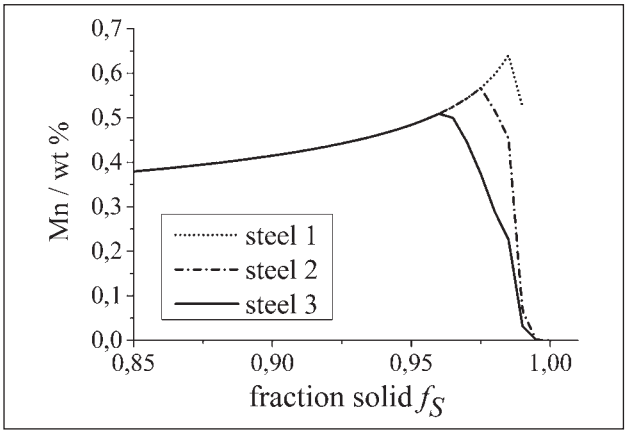

Figure 3 Manganese segregation during silicon steel solidification at a cooling rate of 100 / K min^{-1}

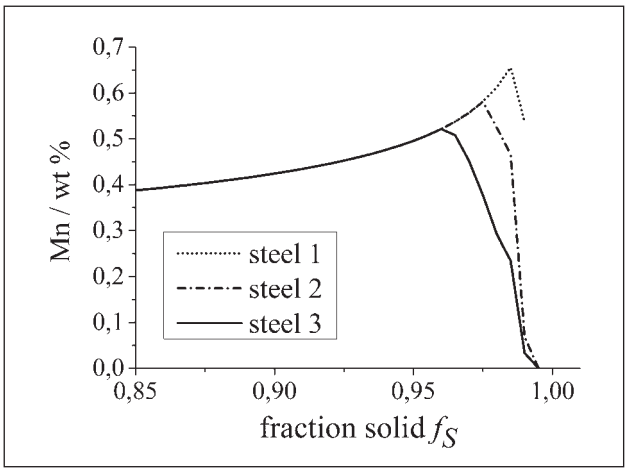

Figure 4 Manganese segregation during silicon steel solidification at a cooling rate of 500 / K min^{-1}

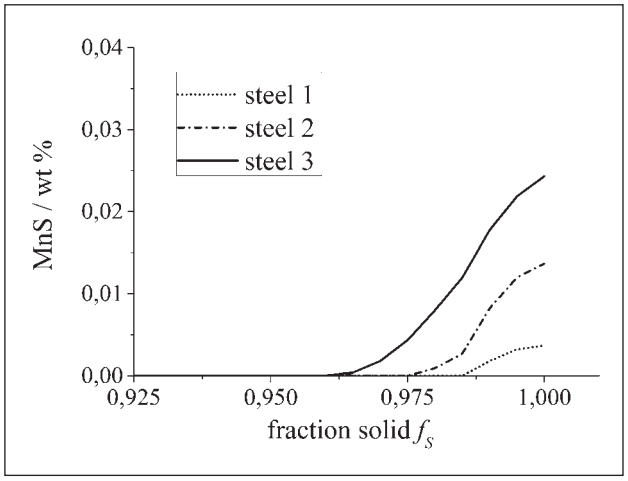

Figure 5 MnS content during silicon steel solidification at a cooling rate of 100 / K min^{-1}

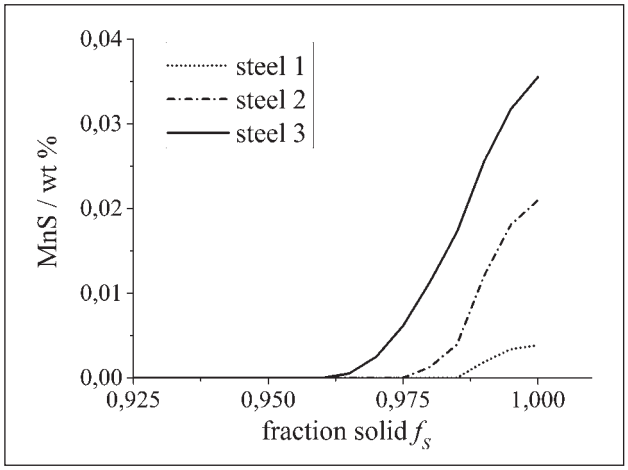

Figure 6 MnS content during silicon steel solidification at a cooling rate of 500 / K min^{-1}

consumed for the production of manganese sulfide. The manganese content in the last portions of liquid steel (steel 1 and 2) tends to zero, signifying that manganese was consumed by sulfur during MnS formation. Figures 5 and 6 illustrate the process of MnS inclusions formation. The calculation results reveal that more manganese sulfide inclusions were produced at the cooling rate 500 / K min^{-1} for steels 1 and 2, whereas in the case of steel 3 the cooling rate did not have any influence.

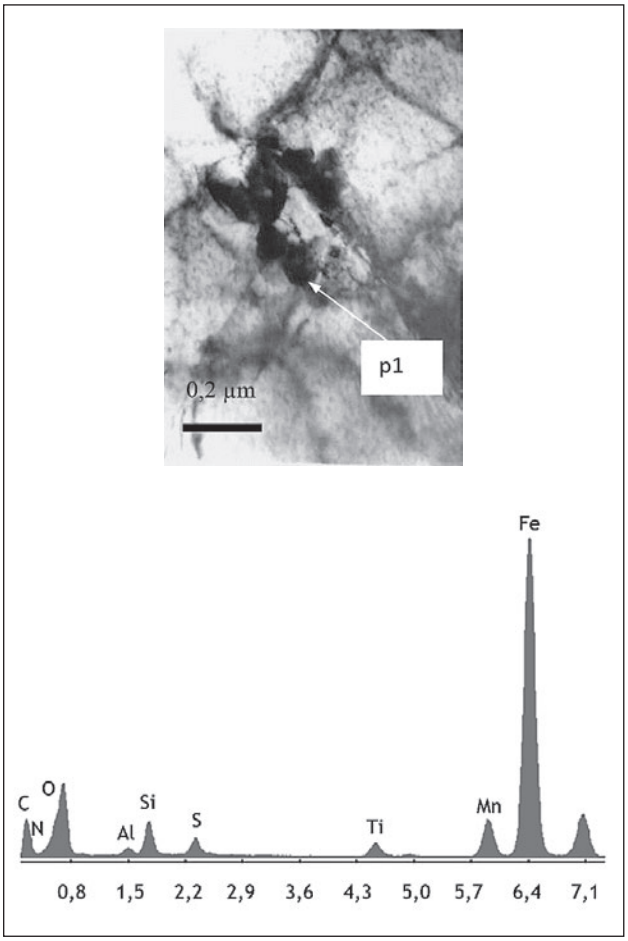

Figure 7 Microstructure obtained in a transmission electron microscope from a silicon steel ingot. The X-ray point microanalysis plot from inclusion area and results of quantitative analysis (Table 2)

STRUCTURE OF SILICA STEEL

For determining the actual chemical composition and size of MnS inclusions produced in the process of high-silicon steel solidification, the microstructure of samples collected from a flat transformer steel ingot was analyzed. The analyses were performed with the use of a transmission electron microscopy and X-ray microanalysis methods. Table 2 / Figure 7.

Table 2 **Chemical composition / %**

Component	et.	at.
C	5,6	19,4
N	0,6	1,8
O	2,2	5,7
Al	1,2	1,9
Si	4,3	6,3
S	2,2	2,8
Mn	7,4	5,5
Ti	2,1	1,8
Fe	71,3	52,7
Cu	3,1	2,0
sum	100	100

The TEM observations revealed that a group of inclusions was present in the ingot sample. The map of elemental distribution in the analyzed inclusion area showed to the presence of Mn, S, Al, Si and N, therefore MnS inclusions produced on the surface of oxide inclusions are likely to be present there as well.

CONCLUSIONS

Calculations were performed with the use of author's software. The obtained results showed that MnS inclusions were formed during solidification and more manganese sulfide inclusions were generated at the cooling rate of 500 K/min. The manganese content in steel turned out to be the parameter which controls the process of MnS separation. The interfacial division coefficient k for Mn (k = 0,77) was considerably higher than for sulfur (k = 0,05), therefore in the course of segregation processes the manganese deficiency occured as a consequence of which sulfide could be produced.

Acknowledgements

The research was performed within the AGH-UST project 11.11.170.318

REFERENCES

[1] N. P. Goss, Patent US (1934), nr 1, 965 559.
[2] J. Wypartowicz, D. Podorska, Hutnik – Wiadomości Hutnicze, 5 (2004), 221-225.
[3] T. Matsumiya, H.Kajioka, S. Mizoguchi, Y. Ueshima, H. Esaka: Mathematical Analysis of Segregation in Continuously cast Slabs, Trans. ISIJ, 24 (1984), 873 - 882.
[4] J. Wypartowicz, D. Podorska, Hutnik - Wiadomości Hutnicze, 6 (2004), 259-264.
[5] D. Kalisz, Modelowanie procesów rafinacji i wprowadzania azotu w stalach elektrotechnicznych, Wydawnictwo Naukowe Akapit, Kraków 2012, s. 120.
[6] D.Kalisz, Termodynamiczna charakterystyka powstawania fazy niemetalicznej w ciekłej stali, Wydawnictwo Naukowe Akapit, Kraków 2013, s. 193.
[7] Z. Liu, K. Gu, K. Cai, ISIJ Int., 42 (2002) 950 – 957.
[8] Z. Ma, D. Janke, ISIJ Int., 38 (1998) 46-52.
[9] Z. Liu, J. Wei, K., ISIJ Int., 42 (2002) 958 – 963.
[10] S. Kobayashi, T. Nagamichi, K. Gunji, Trans. ISIJ, 28 (1988) 543 - 552.
[11] W. Wołczyński, Effect of the back-diffusion onto doublet structure formation and solute redistribution within alloys solidyfying directionally, with or without convection, Polish Academy of Sciences, Institute of Metallurgy and Materials Science, Kraków -2002.
[12] S. Kobayashi, ISIJ Int., 39 (1999), 664-670.
[13] V. Y. Dashevskii, A. M. Katsenelson, N. N. Makarova, K. V. Grigorovitch, V. I. Kashin, ISIJ Int. 43 (2003) 1487-1494.
[14] S. Ban-ya, ISIJ Int. 33 (1993) 2-11.
[15] J. Iwanciw, Arch. Met. And Materials, 49 (2004) 595-609.
[16] B. Kalandyk, M. Starowicz, M. Kawalec, R. Zapała, Metalurgija, 52 (2013) 75-78.
[17] I. Mamuzić, M. Longauerowa, A. Strkalj, Metalurgija 44 (2005) 201-2017.
[18] J. S. Suchy, J. Lelito, B. Gracz, P. L. Żak, China Foundry 9 (2012) 184-190.

Note: The responsible translator for English language: „ANGOS" Translation Office, Kraków, Poland